DOI: 10.1002/((please add manuscript number))
Article type: Communication

Probing the Active Sites of Carbon Encapsulated Cobalt Nanoparticles for Oxygen Reduction

*Xuecheng Yan, Chung-Li Dong, Yu-Cheng Huang, Yi Jia, Longzhou Zhang, Shaohua Shen, Jun Chen, and Xiangdong Yao**

Dr. X. C. Yan, Dr. Y. Jia, Dr. L. Z. Zhang, Prof. X. D. Yao
Queensland Micro- and Nanotechnology Centre, Griffith University
Nathan Campus, QLD 4111, Australia
E-mail: x.yao@griffith.edu.au
Prof. C. L. Dong, Y. C. Huang
Department of Physics, Tamkang University
Tamsui District, New Taipei City 25137, Taiwan
Prof. S. H. Shen
International Research Center for Renewable Energy, State Key Laboratory of Multiphase Flow in Power Engineering, Xi'an Jiaotong University
Xi'an 710049, P. R. China
Prof. J. Chen
Intelligent Polymer Research Institute, ARC Centre of Excellence for Electromaterials Science, AIIM Facility, University of Wollongong
Innovation Campus, Wollongong, NSW 2522, Australia

Keywords: active sites, core-shell structures, single Co species, oxygen reduction reaction

Great effort has been contributed to exploring efficient and cost-effective oxygen reduction reaction (ORR) catalysts for fuel cell applications in the past decades. Now various electrocatalysts can be synthesized for high-performance ORR catalysis. However, the identification of the ORR active sites in many non-precious metal-based catalysts is still difficult. This is due to the heterogeneity and complexity of the catalyst structures. For example, the active site of core-shell ORR electrocatalysts has been a continuously debatable issue, hampering the exploration of new ORR catalysts. Herein, a carbonized Co metal organic framework (Co@C) is used to uncover the ORR active sites in core-shell electrocatalysts. The surface Co particles in the Co@C sample are removed by HCl wash, and the Co cores are removed using an electrochemical activation method. The characterizations reveal that both the samples before and after the electrochemical activation show the existence of single Co species.

The corresponding electrocatalysis test results indicate that neither the surface Co particles nor the encapsulated Co cores influence the ORR performance of the samples. It is deduced that the single Co species coordinated with the nitrogen in the carbon layers of the core-shell catalysts are the actual ORR active sites.

Fuel cells and associated clean energy technologies provide feasible solutions in tackling the existing energy shortage and environmental pollution issues. However, the sluggish oxygen reduction reaction (ORR) on the cathode of the fuel cell considerably impedes its output energy efficiency. At present, the expensive platinum (Pt) based materials are used to accelerate the ORR process. This is not a long-term development strategy because of the low abundance of the Pt resources. Consequently, the exploration of non-precious metal based ORR electrocatalysts has attracted increasingly attentions over the last decade. Particularly, transition metals (such as Fe, Co and Ni) coupled with various carbon materials have been intensively investigated due to their multiple advantages, including low cost, high performance as well as excellent durability.[1-4] For example, a series of significant investigations on developing carbon materials anchored/encapsulated Fe or Co particles for efficient ORR catalysis have been reported since 2009.[5-7] These pioneering studies have triggered the recent thorough exploration of non-noble metals as alternative ORR electrocatalysts. Subsequently, enormous researches have been devoted to exploiting various Co or Fe based materials for catalyzing the ORR. Typical examples include cobalt/iron oxide coupled with graphene,[3,8-11] carbon nanotubes coupled with cobalt/iron nanoparticles,[12-16] and carbon encapsulated cobalt/iron nanoparticles.[17-19]

The ORR performance of the resulting non-precious metal catalysts shows remarkable improvement, for instance, some of them are comparable or even outperformed the commercial Pt/C in alkaline conditions.[20-22] However, the identification of the active sties in these carbon coupled Fe/Co catalysts remains a complicated issue. Particularly, extensive research has been

focused on revealing the ORR active sites in carbon encapsulated Fe/Co composites.[2,23-26] This is because the metal cores are not directly contacting with the electrolyte, but the core-shell catalysts still show greatly enhanced ORR activity. The significance and representative investigations on identifying the ORR active sites in core-shell-structured catalysts can be found in the high-level work summarized in Table S1 (Supporting Information). As can be seen, the ORR active sites in these core-shell catalysts are still controversial and not clear. Since the metal particles are wrapped by the graphitic layers, and they could not contact with the electrolyte or oxygen directly, thus they should not be the ORR active sites. It is assumed that the active sites are the outside carbon layers activated by the inner metal cores, or the interfaces between the carbon and metal particles,[25] but these conclusions are lack of solid proofs. In this regard, direct experimental evidences are highly desirable to uncover the veil of the active sites in these materials. In the past, the influence of atomic metal species (defects coordinated with atomic metals) on electrocatalysis in most metal-carbon catalysts have been ignored/underestimated because normal characterizations could not detect them. With the advancement of modern characterization techniques, recent investigations show that single metal species play crucial roles on various electrochemical reactions. For instance, single Ni species are responsible for the hydrogen evolution reaction (HER) in a Ni-coordinated defective graphene,[27] atomic Co species with tetrahedral coordination are active for the ORR.[28-30] Therefore, the actual influence of the atomic metal species on the surface of carbon shells for electrocatalysis should be considered and studied.

In this work, we select a Co containing metal organic framework (Co-MOF) as the precursor to probe the real ORR active sites of carbon encapsulated Co nanoparticles. Firstly, the Co-MOF was prepared by the reported method.[31] Subsequently, this Co-MOF sample was carbonized with dicyandiamide at 850 °C for 2 h under a nitrogen atmosphere (the carbonized sample before acid washing was denoted as Co@C-BW). The Co particles on the surface of the carbonized sample were removed by HCl acid wash. The resulting sample was denoted

as Co@C. Afterwards, we used an electrochemical activation method to further remove the Co nanoparticles encapsulated by the carbon layers (the sample activated with 8000 cyclic voltammetry (CV) cycles was denoted as Co@C-A). It is shown that the samples before and after the electrochemical activation exhibit almost the same ORR performance, and the surface Co particles hardly influence the ORR. The transmission electron microscopy (TEM) confirms that most of the Co cores have been removed after the electrochemical activation. It means that the ORR active sites may not be the surface Co particles or the encapsulated Co cores. Remarkably, the high-angle annular dark-field imaging (HAADF)-scanning transmission electron microscope (STEM) directly observed the existence of single Co species in both the Co@C and Co@C-A samples. The corresponding extended X-ray absorption fine structure (EXAFS) and X-ray absorption near-edge structure (XANES) characterizations also confirm that the sample Co@C-A shows the presence of single Co species, which are coordinated with the nitrogen in the carbon layers. These single Co atoms are believed to play vital roles for the ORR catalysis, which are more likely to be the actual active sites for the electrocatalysis in carbon encapsulated Co materials. For comparison, we synthesized a nitrogen doped carbon (N-C) using Zn-MOF-74 as the precursor, it shows that the N-C is much less active for the ORR than that of the Co@C. This further suggests that the doped nitrogen is not the ORR active site, and the single Co species should be responsible for catalyzing the ORR in the prepared samples. The Co-MOF was prepared *via* a facile mixed solvent method at 65 °C under an atmospheric pressure, the experimental details can be found in the Experimental Section in Supporting Information. Its structure and magnified optical photo are shown in **Figure 1**. After carbonizing the Co-MOF with dicyandiamide at the mass ratio of 1 to 2 at 850 °C for 2 h, a sample with distinct core-shell structures is obtained (illustrated and confirmed by the TEM image, shown in Figure 1). It can be observed from Figure 1 that the Co core is wrapped by multiple layers of graphitic carbon. Apparently, it is not viable to remove the inner Co cores by a normal acid

wash method, since the acid could not contact with them directly. In this study, we applied an electrochemical activation method to remove the Co cores, which is a commonly used method to dissolve metal particles encapsulated by carbons.[31,32] We can see from Figure 1 that the Co core has been removed after the electrochemical activation treatment, and the layered graphitic structure is well-maintained.

The X-ray powder diffraction (XRD) pattern of the synthesized Co-MOF can be seen in Figure S1 (Supporting Information). After carbonization at 850 °C for 2 h, a sample with distinct Co particles is obtained (Figure S2, Supporting Information). We thereafter used 2 M HCl to remove the surface Co nanoparticles. As shown in **Figure 2**a, compared with the sample Co@C-BW, the Co particles in the HCl washed sample Co@C present a more uniform size distribution. The majority of the Co particles in the Co@C are around 15 nm in diameter, as revealed by the histogram in Figure S3 (Supporting Information). The energy-dispersive X-ray spectroscopy (EDS) mapping was used to reveal the elemental distributions of the Co@C sample. It can be observed from Figure S4 (Supporting Information) that the Co particles are homogeneously distributed in the carbon. The uniform nitrogen in the Co@C should come from the dicyandiamide during the carbonization process, which is effective in capturing single Co species.[29] In addition, we used X-ray photoelectron spectroscopy (XPS) analyzed the surface Co in the Co@C-BW and Co@C samples. The corresponding results in Figure 2b and Table S2 (Supporting Information) show that the surface Co in the Co@C-BW sample is decreased from 0.85 at% to nearly zero (below the XPS detection limit) after the acid treatment. This suggests that all the surface Co particles have been removed after the HCl washing. However, the carbon encapsulated Co nanoparticles core-shell structures are well retained (Figure 2a, inset). The inductively coupled plasma (ICP) test results further confirm the sharp decrease of the Co content in the Co@C-BW after HCl wash, from 17.97 wt% to 7.34 wt%. Afterwards, we used an electrochemical activation method to further dissolve the Co cores. Specifically, we firstly dropped the Co@C sample onto a rotating disk electrode (RDE). Then this sample was

activated under the CV range of 0.1 to 1.1 V (*vs*. RHE) in a 0.5 M H_2SO_4 solution. A graphite rod is used as the counter electrode during the activation and ORR measurement. It can be seen from Figure 2c that the encapsulated Co cores have been removed after activation for 8000 CV cycles. The possible reason is that a small part of amorphous carbons in the shells are being oxidized and etched under the activation conditions. This is verified by the corresponding Raman test results in Figure S5 (Supporting Information), since the activated sample Co@C-A shows a higher graphitic degree than that of the Co@C sample. Therefore, valid channels will be created to allow the H_2SO_4 electrolyte to react with the encapsulated Co nanoparticles (Figure 2d and e). The produced channels in the graphitic layers of the Co@C sample can be clearly seen from Figure 2e. Apparently, this will allow the H_2SO_4 solution to directly contact and react with the Co cores, which should be the reason accounting for the removal of the carbon wrapped Co particles. The XPS spectrum in Figure S6 (Supporting Information) shows that no Co signal is detected in the activated sample Co@C-A, but a very strong F peak is observed. This F signal is from Nafion as it is used in preparing the electrode ink. The accurate Co content in the Co@C-A is identified to be 2.24 wt% by the ICP test, which further supports the above characterizations and discussions.

The single Co species were examined using aberration-corrected high-resolution TEM (AC-TEM). From the high-angle annular dark-field imaging (HAADF) in Figure 2f, we can observe that the Co@C sample shows a very distinct Co core with the particle size around 12 nm. Particularly, very clear single Co species (cycled white dots) can be found in the carbon layers of this sample. This fully proves the existence of single Co species on the surface of Co@C. The sample after the electrochemical activation for 8000 cycles was tested by the HAADF-STEM as well. From Figure 2g, we can observe a hollow structure in the Co@C-A sample, with abundant single Co species (cycled white dots) decorated on the shell of the carbon layers. Apparently, both the samples before and after the electrochemical activation show the presence of single Co species. We thereafter used X-ray absorption spectroscopy (XAS) measurements

to further study the structures of the single Co species at atomic levels in the Co@C-BW, Co@C and Co@C-A samples. The X-ray absorption near-edge structure (XANES) spectra of the Co@C-BW and Co@C samples in Figure 2h show that most of the Co species are metallic Co, since the white line peaks of the Co@C-BW and Co@C are very close to that of the reference sample Co foil (Figure 2h). This is reasonable because compared to the surface Co particles and the encapsulated Co cores, the percentage of the single Co species is very low. Therefore, the majority of the XANES signal is from the bulk Co nanoparticles. The corresponding extended X-ray absorption fine structure (EXAFS) test results of the Co@C-BW and Co@C samples in Figure 2i further confirm this conclusion. In contrast, the sample Co@C-A that after the electrochemical activation shows distinct single Co species peaks in both the XANES and EXAFS spectra (Figure 2h and 2i). For example, the intensity of the Co-Co peak located at 2.2 Å is decreased sharply in the Co@C-A, compared to the Co@C sample. This further suggests that most of the Co cores have been removed, with seldom Co clusters/particles residuals. Impressively, a distinct Co-N/Co-C peak at 1.4 Å is detected in the *R*-space spectrum of the Co@C-A sample (Figure 2i), indicating the atomic dispersion of the Co species in the carbon layers. The EXAFS fittings were conducted to identify the structural parameters and the specific chemical configurations of the Co species in the prepared samples (**Figure 3**). For the samples Co@C-BW and Co@C, only Co-Co path can be gained due to the existence of a large amount of Co particles/cores (Figure 3a and b). The corresponding fitting parameters given in Table S3 (Supporting Information) suggest that the coordination number for these two samples is 11. Although no single Co species are found from the fitted EXAFS *R*-space curves, the high resolution XPS N 1s fittings for the surface nitrogen in the Co@C-BW and Co@C samples show the possible coordination of Co species with the nitrogen (Figure S7, Supporting Information). However, for the activated sample Co@C-A, single Co species can be

fitted (Figure 3c), and the gained coordination number of Co-N within the Co@C-A is 4, indicating that the Co atom is coordinated by four N atoms (illustrated by Figure 3d). This result is consistent with the reported work on single Co species to catalyze the ORR.[29,30] The AC-TEM and XAS characterizations show robust evidences on the presence of single Co species in the Co@C and Co@C-A samples, and these single Co species are very possible play important roles on the ORR catalysis.

Afterwards, we examined the role of the Co nanoparticles/species in the prepared samples on electrocatalysis by evaluating their oxygen reduction performance. The ORR is tested in an oxygen-saturated 0.1 M KOH electrolyte using a rotating disk electrode. We can see from **Figure 4**a that with the commonly used catalyst loading of 0.32 mg cm^{-2}, the ORR activity of the Co@C is similar to that of the reported Co-based catalysts.[3,10] Considering the efficiency of the electrochemical activation, we used a reduced catalyst loading of 0.04 mg cm^{-2} to remove the Co cores as many as possible. From Figure 4a, it can be observed that even at this low catalyst loading, the sample Co@C still shows very obvious ORR activity, as compared with the bare glassy carbon electrode. Subsequently, we activated the Co@C sample with the loading of 0.04 mg cm^{-2} at different CV cycles. The ORR performance of the Co@C activated in 0.5 M H_2SO_4 with 2000, 4000, 6000 and 8000 cycles is presented in Figure 4b. Remarkably, all the four samples with different activation cycles show very similar ORR activity to that of the un-activated sample Co@C (Figure 4b). The corresponding TEM images of the four activated samples can be seen from Figure 4c-f. Apparently, the encapsulated Co particles in the Co@C sample were gradually removed with the increase of the activation cycle. For example, after 2000 cycles, some Co cores have been partially or fully removed, but we can still observe untouched Co particles (Figure 4c). When the activation cycle reaches 4000, the majority of the encapsulated Co particles have been removed, only left very small amount of Co nanoparticles with the size around 5 nm (Figure 4d). As expected, no big Co cores/particles were found in the TEM images of the Co@C sample after

activated for 6000 and 8000 cycles (Figure 4e and f). This means that almost all the wrapped Co nanoparticles have been removed after 6000 cycles. Combine the ORR activity of the activated samples in Figure 4b and the corresponding TEM results in Figure 4c-f, we can reasonably deduce that the graphitic carbon encapsulated Co nanoparticles are not the active sites for the ORR. Meanwhile, the calculated turnover frequencies (TOFs) of the Co@C and Co@C-A samples at the potential of 0.7 V (*vs*. RHE in Figure 4b) are 0.122 s^{-1} and 0.395 s^{-1}, respectively. It is obvious that the TOF is higher when the Co content is lower, further showing that the Co particles/clusters are not active for the ORR. Besides, the ORR performance of the Co@C-BW sample (without HCl wash) was measured as well. It shows from Figure S8 (Supporting Information) that the surface Co particles are not active for the ORR either, since the ORR activity of the Co@C and Co@C-BW samples is quite similar. The slightly higher current density of the Co@C-A may be attributed to its marginally higher conductivity, as indicates in the electrochemical impedance test results in Figure S9 (Supporting Information). In addition, the synthesized nitrogen doped carbon (N-C) using Zn-MOF-74 as the precursor exhibits much less active for the ORR than that of the Co@C (Figure S10, Supporting Information), further indicating that the doped nitrogen is not active for the ORR, and the single Co species should be contributed to the excellent ORR performance of the prepared samples. From the above characterizations and discussions on the Co@C and Co@C-A samples, the single Co species are contained in both samples, which should be the actual ORR active sites. In addition, from the previous reported work on single metal atoms catalysis, we can also deduce that the single Co species coordinated with the nitrogen in the carbon layers of the resulting catalysts are crucial to the ORR.

In addition, the ORR polarization curves of the Co@C-A sample were measured from 400 to 2500 rpm in an oxygen-saturated 0.1 M KOH solution. The corresponding ORR current is increased with the increase of the rotation speed (Figure S11, Supporting

Information), implying that the ORR is a diffusion-controlled reaction process. Thereafter, the stability of the Co@C-A sample was evaluated using the amperometric *i–t* method. For better comparison, both the Co@C-A and the commercial Pt/C were tested in an oxygen-saturated 0.1 M KOH solution. It can be found from Figure 4g that the Co@C-A sample is much more stable than that of the Pt/C. For example, the ORR activity of the Co@C-A could maintain 92.2% after continuous measurement of 20000 s. However, the Pt/C only retained 80.6% of its initial current. These results show that the single Co species could anchor on the outside carbon layers strongly, resulting in the excellent ORR durability of the Co@C-A sample.

In summary, we synthesized a kind of Co-based core-shell material by carbonizing a Co-MOF. The unique configurations of the carbonized sample Co@C provides an ideal model for understanding the oxygen reduction reaction active sites of carbon encapsulated metal electrocatalysts. The surface Co particles were removed by thoroughly washing in a 2 M HCl acid solution. The wrapped Co cores were successfully removed using an electrochemical activation method in a 0.5 M H_2SO_4 electrolyte. Remarkably, the ORR performance of the resulting sample was not affected by the removal of the surface Co nanoparticles or the Co cores. The corresponding aberration-corrected high-resolution TEM and X-ray absorption spectroscopy measurements reveal that both the samples before and after the activation show the presence of single Co species, which are believed to act as the active sites and play vital roles in promoting the ORR. This work provides new insights and opens a novel avenue to probe the active sties of electrocatalysts with core-shell structures.

Experimental Section

See Supporting Information section for details of the Sample Preparation, Characterizations and Electrochemical Measurement.

Supporting Information

Supporting Information is available from the Wiley Online Library or from the author.

Acknowledgements

The authors would like to thank Australian Research Council (ARC DP170103317) for financial support during the course of this work.

Conflict of Interest

The authors declare no conflict of interest.

Received: ((will be filled in by the editorial staff))
Revised: ((will be filled in by the editorial staff))
Published online: ((will be filled in by the editorial staff))

References

[1] Y. Nie, L. Li, Z. Wei, *Chem. Soc. Rev.* **2015**, *44*, 2168.

[2] Y. Hu, J. O. Jensen, W. Zhang, L. N. Cleemann, W. Xing, N. J. Bjerrum, Q. Li, *Angew. Chem. Int. Ed.* **2014**, *53*, 3675.

[3] T. Odedairo, X. Yan, J. Ma, Y. Jiao, X. Yao, A. Du, Z. Zhu, *ACS Appl. Mater. Interfaces* **2015**, *7*, 21373.

[4] X. Yan, Y. Jia, X. Yao, *Chem. Soc. Rev.* **2018**, *47*, 7628.

[5] M. Lefèvre, E. Proietti, F. Jaouen, J.-P. Dodelet, *Science* **2009**, *324*, 71.

[6] Y. Liang, Y. Li, H. Wang, J. Zhou, J. Wang, T. Regier, H. Dai, *Nat. Mater.* **2011**, *10*, 780.

[7] G. Wu, K. L. More, C. M. Johnston, P. Zelenay, *Science* **2011**, *332*, 443.

[8] Q. He, Q. Li, S. Khene, X. Ren, F. E. López-Suárez, D. Lozano-Castelló, A. Bueno-López, G. Wu, *J. Phys. Chem. C* **2013**, *117*, 8697.

[9] B. Zheng, J. Wang, F.-B. Wang, X.-H. Xia, *J. Mater. Chem. A* **2014**, *2*, 9079.

[10] Y. Tong, P. Chen, T. Zhou, K. Xu, W. Chu, C. Wu, Y. Xie, *Angew. Chem. Int. Ed.* **2017**, *56*, 7121.

[11] K. Parvez, S. B. Yang, Y. Hernandez, A. Winter, A. Turchanin, X. L. Feng, K. Mullen, *ACS Nano* **2012**, *6*, 9541.

[12] Z. S. Yin, T. H. Hu, J. L. Wang, C. Wang, Z. X. Liu, J. W. Guo, *Electrochim. Acta* **2014**, *119*, 144.

[13] S. Dou, X. Li, L. Tao, J. Huo, S. Wang, *Chem. Commun.* **2016**, *52*, 9727.

[14] A. Morozan, S. Campidelli, A. Filoramo, B. Jousselme, S. Palacin, *Carbon* **2011**, *49*, 4839.

[15] Y. Liang, H. Wang, P. Diao, W. Chang, G. Hong, Y. Li, M. Gong, L. Xie, J. Zhou, J. Wang, T. Z. Regier, F. Wei, H. Dai, *J. Am. Chem. Soc.* **2012**, *134*, 15849.

[16] R. Cao, R. Thapa, H. Kim, X. Xu, M. Gyu Kim, Q. Li, N. Park, M. Liu, J. Cho, *Nat. Commun.* **2013**, *4*, 2076.

[17] A. Aijaz, J. Masa, C. Rösler, W. Xia, P. Weide, A. J. R. Botz, R. A. Fischer, W. Schuhmann, M. Muhler, *Angew. Chem. Int. Ed.* **2016**, *55*, 4087.

[18] H. T. Chung, J. H. Won, P. Zelenay, *Nat. Commun.* **2013**, *4*, 1922.

[19] D. Deng, L. Yu, X. Chen, G. Wang, L. Jin, X. Pan, J. Deng, G. Sun, X. Bao, *Angew. Chem. Int. Ed.* **2013**, *52*, 371.

[20] X. Yan, Y. Jia, J. Chen, Z. Zhu, X. Yao, *Adv. Mater.* **2016**, *28*, 8771.

[21] X. Yan, Y. A. Jia, L. Zhang, M. T. Soo, X. Yao, *Chem. Commun.* **2017**, *53*, 12140.

[22] M. Zhang, Q. Dai, H. Zheng, M. Chen, L. Dai, *Adv. Mater.* **2018**, *30*, 1705431.

[23] Y. Hu, L. Zhong, J. O. Jensen, Q. Li, *Asia-Pac. J. Chem. Eng.* **2016**, *11*, 382.

[24] Y. Hu, J. O. Jensen, W. Zhang, S. Martin, R. Chenitz, C. Pan, W. Xing, N. J. Bjerrum, Q. Li, *J. Mater. Chem. A* **2015**, *3*, 1752.

[25] K. Strickland, E. Miner, Q. Jia, U. Tylus, N. Ramaswamy, W. Liang, M.-T. Sougrati, F. Jaouen, S. Mukerjee, *Nat. Commun.* **2015**, *6*, 7343.

[26] J. A. Varnell, E. C. M. Tse, C. E. Schulz, T. T. Fister, R. T. Haasch, J. Timoshenko, A. I. Frenkel, A. A. Gewirth, *Nat. Commun.* **2016**, *7*, 12582.

[27] L. Zhang, Y. Jia, G. Gao, X. Yan, N. Chen, J. Chen, M. T. Soo, B. Wood, D. Yang, A. Du, X. Yao, *Chem* **2018**, *4*, 285.

[28] X. X. Wang, D. A. Cullen, Y.-T. Pan, S. Hwang, M. Wang, Z. Feng, J. Wang, M. H. Engelhard, H. Zhang, Y. He, Y. Shao, D. Su, K. L. More, J. S. Spendelow, G. Wu, *Adv. Mater.* **2018**, *30*, 1706758.

[29] Y. Han, Y.-G. Wang, W. Chen, R. Xu, L. Zheng, J. Zhang, J. Luo, R.-A. Shen, Y. Zhu, W.-C. Cheong, C. Chen, Q. Peng, D. Wang, Y. Li, *J. Am. Chem. Soc.* **2017**, *139*, 17269.

[30] P. Yin, T. Yao, Y. Wu, L. Zheng, Y. Lin, W. Liu, H. Ju, J. Zhu, X. Hong, Z. Deng, G. Zhou, S. Wei, Y. Li, *Angew. Chem. Int. Ed.* **2016**, *55*, 10800.

[31] L. Zhang, J. M. T. A. Fischer, Y. A. Jia, X. Yan, W. Xu, X. Wang, J. Chen, D. Yang, H. Liu, L. Zhuang, M. Hankel, D. J. Searles, K. Huang, S. Feng, C. L. Brown, X. Yao, *J. Am. Chem. Soc.* **2018**, *140*, 10757.

[32] L. Fan, P. F. Liu, X. Yan, L. Gu, Z. Z. Yang, H. G. Yang, S. Qiu, X. Yao, *Nat. Commun.* **2016**, *7*, 10667.

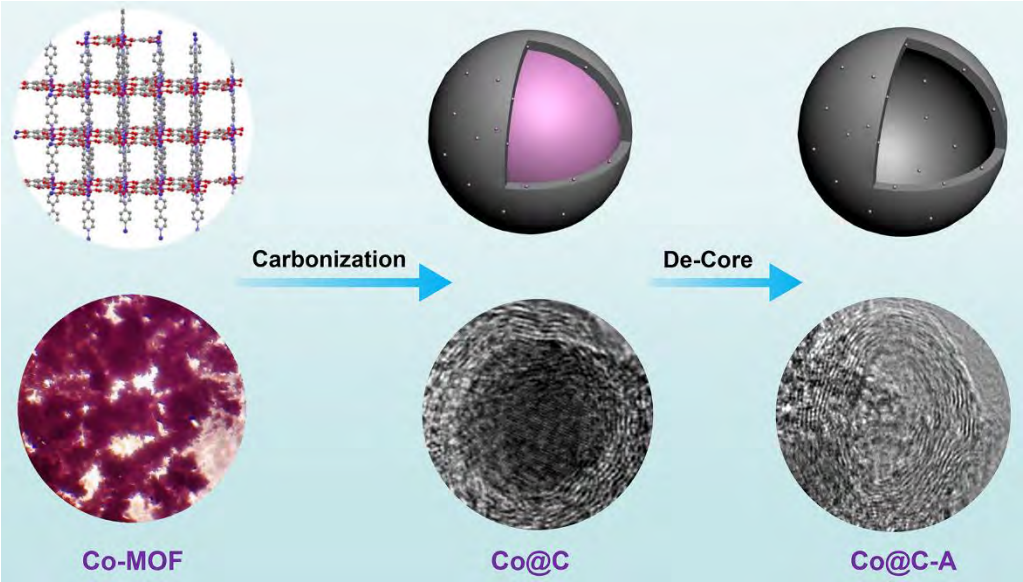

Figure 1. Schematic showing the preparation of Co-based core-shell sample, and the removal of the Co cores.

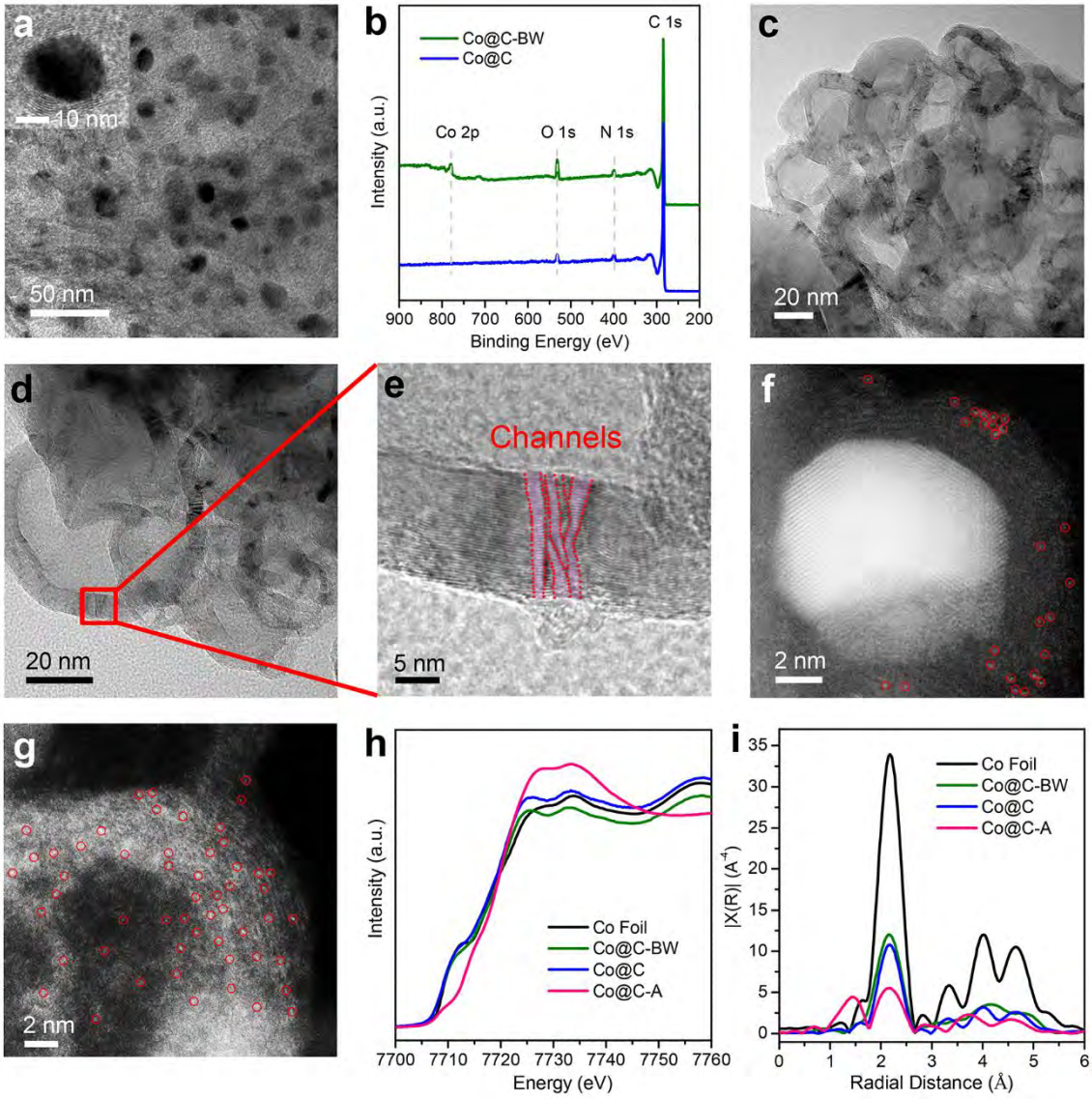

Figure 2. a) TEM image of the Co@C sample (inset: magnified view of the core-shell structure); b) XPS survey spectra of the Co@C-BW and Co@C samples; c) TEM image of the Co@C-A sample showing the hollow carbon structures; d and e) TEM image and magnified view of the Co@C-A sample showing the channels for electrolytes access; f) HAADF-STEM image of Co@C sample; g) HAADF-STEM image of Co@C-A sample; h) Co K-edge XANES spectra of Co@C-BW, Co@C and Co@C-A, and the reference sample Co foil; i) *k*3-weighted $\chi(k)$-function of the EXAFS spectra of Co@C-BW, Co@C and Co@C-A, and the reference sample Co foil. The single Co species are highlighted by red cycles in (f) and (g).

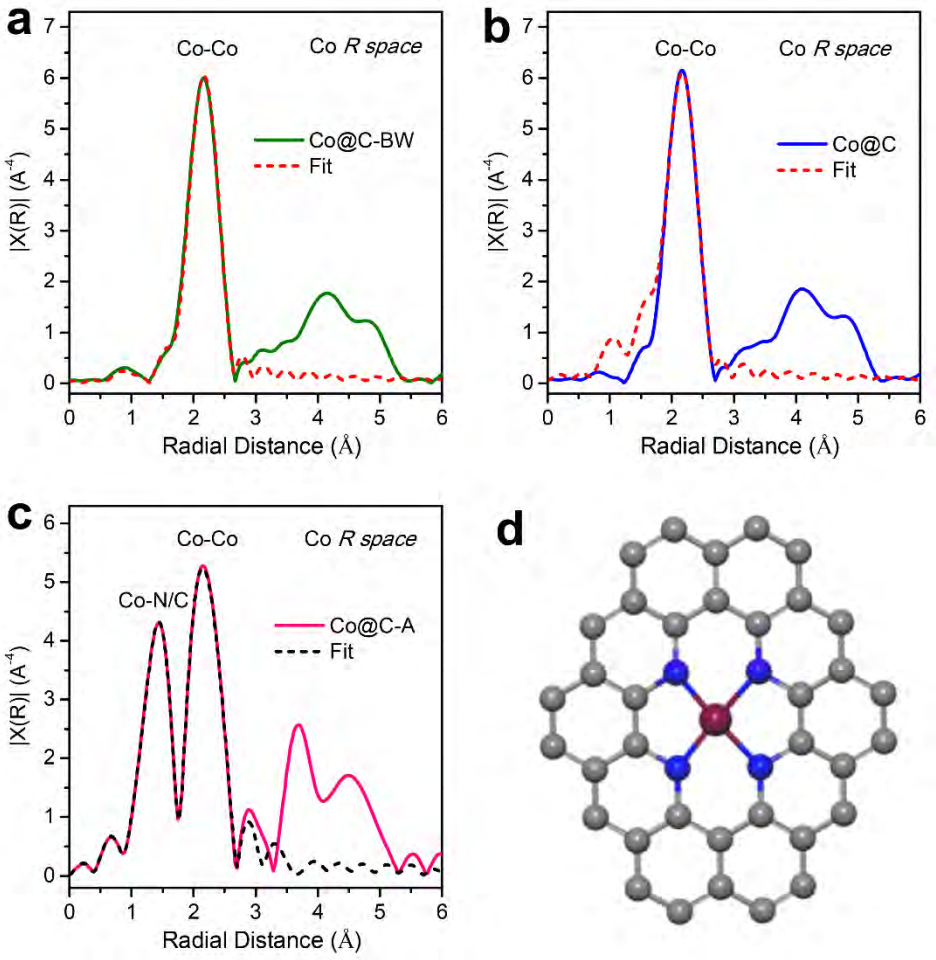

Figure 3. The EXAFS *R*-space fitting curves of the prepared samples: a) Co@C-BW; b) Co@C and c) Co@C-A; d) Schematic model of Co-N coordination in Co@C-A, Co: dark red, N: blue, C: gray.

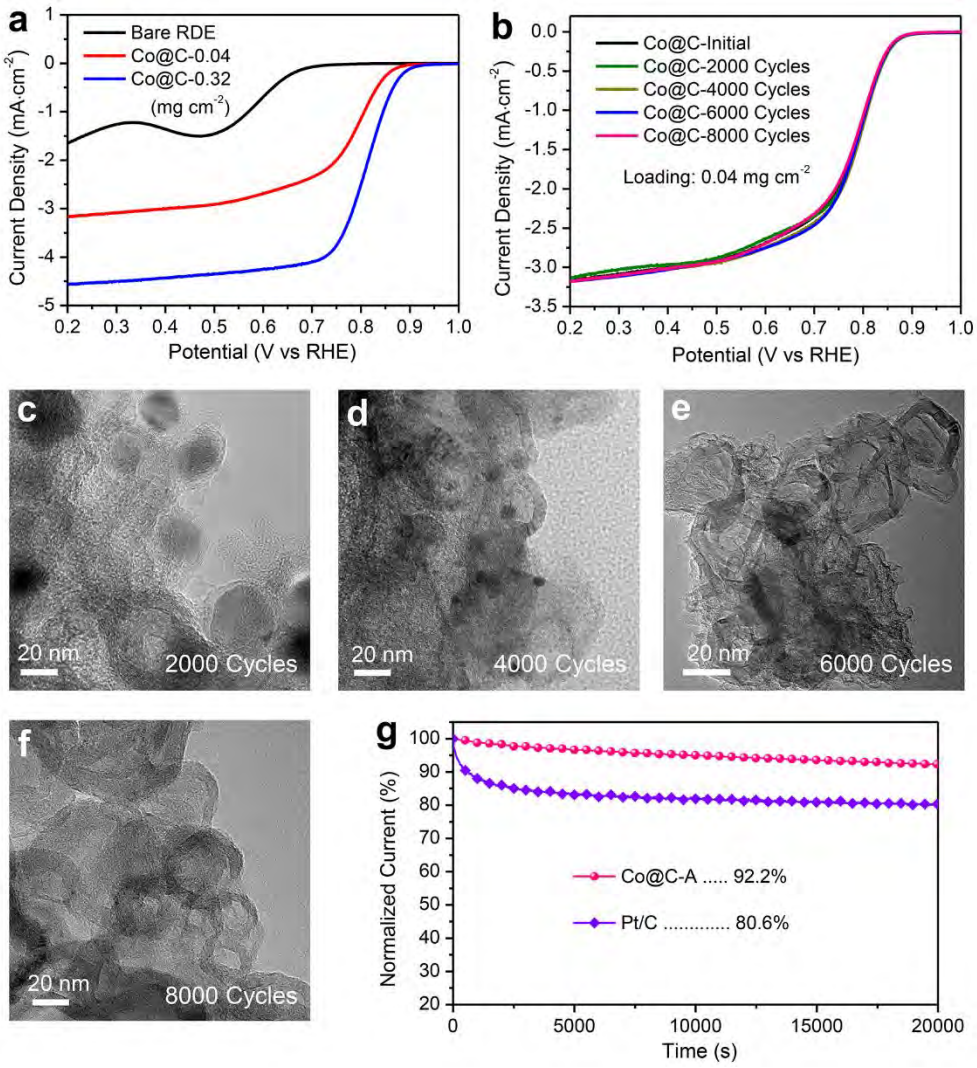

Figure 4. a) LSV curves of the Co@C sample with different catalyst loadings, the bare RDE was tested as a reference; b) ORR performance of the Co@C sample activated under different CV cycles; c-f) TEM images of the Co@C sample activated under various CV cycles; g) *i-t* stability of the Co-@C-A and the commercial Pt/C. The ORR was measured in an oxygen-saturated 0.1 M KOH electrolyte with the rotation speed of 1600 rpm.